Vortex Decay in Quasi-2D MHD Ducts:
Application to Kármán Vortex Streets Behind Turbulence Promoters

A. H. A. Hamid[1,2], W. K. Hussam[1] and G. J. Sheard[1]

[1]The Sheard Lab, Department of Mechanical and Aerospace Engineering, Monash University, Victoria 3800, Australia

[2]Faculty of Mechanical Engineering, Universiti Teknologi MARA, 40450 Selangor, Malaysia

Abstract

A vortex decay model for predicting temporal evolution of peak vorticity in a wake behind a cylinder is presented. Where the wake vortices are in stable region, results have shown that the correlation has a good capability of predicting temporal evolution of peak vorticity within an advecting vortex across a wide range of flow parameters. The correlation is also generalized to predict the dacay behaviour of wake vortices in a class of magnetohydrodynamic duct flows. Comparison with published data demonstrates the capability of this model in predicting vortex strength with a relative standard error of less than 2%.

Introduction

The vortex street generated from a two-dimensional (2-D) bluff body has always been a subject of interest due to its academic and practical importance in engineering [11]. 2-D vortex streets have further been shown to contribute significantly to improving transverse convective heat transport in magnetohydrodynamic (MHD) duct flow, and thus the improved understanding of the transport and decay of vortices in these flows is crucial for the design of efficient heat transport systems in high-magnetic-field applications [4]. When the fluid is electrically conducting and subjected to a strong magnetic field, the decay of wake vortices perpendicular to the field is accelerated via Joule dissipation (due to the Lorentz forces induced by magnetic field) and will experience exponential decay [12]. This fact was confirmed by the experimental investigation by [3], where they measured the vorticity of a cylinder wake at four different streamwise locations. Their results revealed that the vortex intensity decayed much faster at Hartmann number $Ha = 1200$ than at $Ha = 500$ as the vortices advected downstream. They concluded that the vortex energy dissipates by Hartmann braking rather than via a cascade down towards smaller structures, which is a prominent feature of MHD flow as compared to pure hydrodynamic flow. When the Hartmann number is increased above a critical value, the shedding is completely inhibited [5].

The decay rate of vorticity is also influenced by the conductivity of the Hartmann walls. For perfectly insulating walls, the characteristic decay time of vorticity is dependent on Hartmann braking with scale proportional to Re/Ha [2]. A numerical investigation by [5] found that for high Reynolds and Hartmann numbers, the viscous diffusion term can be neglected. Thus the decay of peak vorticity magnitude of an individual wake vortex is described by the Hartmann friction term only, i.e. Re/Ha as suggested by previous theory.

In summary, considerable research has been done on the behavior of wake vortices, with and without a magnetic field. However, little is known about the decaying core vorticity behavior. In the current work, the decay of wake vortices under various flow parameters are quantitatively analyzed. The aim is to devise a correlation describing the decay behaviour of cylinder wake peak vorticity under the influence of a strong magnetic field.

Analytical Solution for a Line Vortex Decay

From [5], the quasi-two-dimensional vorticity transport equation for an incompressible flow of an electrically conducting fluid between two plates subjected to a uniform strong magnetic field in the out-of-plane direction is given in dimensionaless form as:

$$\frac{D\xi}{Dt} = \nabla^2\xi - 2Ha\,\xi, \tag{1}$$

where ξ is vorticity, t is time, D/Dt the material derivative, ∇ the gradient operator, the Hartmann number $Ha = Ba\sqrt{\sigma/\rho\nu}$, where B, a, σ, ρ and ν are the applied magnetic field, out-of-plane duct height, magnetic permeability, density and kinematic viscosity of the liquid metal, respectively. The length, time and vorticity are scaled by gap height, a, a^2/ν and ν/a^2 respectively. In cylindrical coordinates, this is rewritten as

$$\frac{D\xi}{Dt} = \frac{\partial^2\xi}{\partial r^2} + \frac{1}{r}\frac{\partial\xi}{\partial r} - 2Ha\,\xi, \tag{2}$$

where r is the radial coordinate.

Equation (2) can be transformed using $\xi(r,t) = e^{(-2Ha\,t)}\xi_1(r,t)$ to give $\partial\xi_1/\partial t = \partial^2\xi_1/\partial r^2 + (1/r)\partial\xi_1/\partial r$ [7]. The solution to this equation is exactly the Lamb–Oseen vortex solution, where the vorticity field is given by $\xi = \Gamma/\pi r_c^2 e^{(-r^2/r_c^2)}$. Here Γ represents the initial amount of circulation contained in an infinitesimal filament. The time variation of the core radius is described by $r_c = \sqrt{4\nu\tau}$, where $\tau = t + t_0$ is the time since the vorticity field is initially concentrated at the origin. It is instructive to also introduce the peak vorticity in this profile, which appears at $r = 0$, $\xi_p = \Gamma/(\pi r_c^2)$. Using the present scaling, the core radius expression non-dimensionalizes to $r_c = \sqrt{4\tau}$ and the peak vorticity to $\xi_p = \Gamma/(4\pi\tau)$. The vortex core radius at an arbitrary time t_0 is defined as $r_0 = \sqrt{4t_0}$. The analytical solution for a Lamb–Oseen peak vorticity is then given by

$$\xi_{1,p} = \frac{\Gamma}{\pi}\left(\frac{1}{4t + r_0^2}\right). \tag{3}$$

Correspondingly the solution for a line vortex decaying in a quasi-2D flow can be expressed as

$$\xi_p = \frac{\Gamma}{\pi}\left(\frac{1}{4t + r_0^2}\right)e^{-2Ha\,t}. \tag{4}$$

Numerical Method and Validation

The system of interest is a circular cylinder confined by a rectangular duct (refer figure 1). The axis of the cylinder is parallel to the spanwise direction and perpendicular to the flow direction. Here lengths are normalized using the half channel width, L. A homogeneous magnetic field with a strength B is imposed parallel to the cylinder axis. A quasi-two-dimensional model proposed by [13] (later known as SM82) has been employed in the current work. This model is derived by averaging the flow
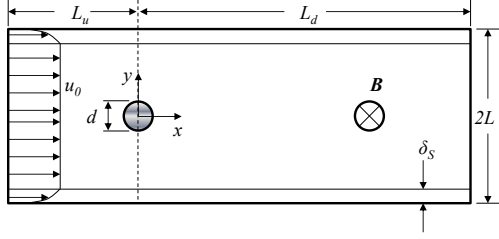
Figure 1. Schematic diagram of numerical domain. The shaded area indicates cylinder of infinite extension along the z-axis with diameter d.

quantities along the magnetic field direction and has been verified against 3D results [9, 10]. It has been applied in many previous works, for example by [5] and [4] due to its accuracy despite its simplicity. Under this model the non-dimensional magnetohydrodynamic equations of continuity and momentum reduce to

$$\nabla \cdot \mathbf{u}_\perp = 0, \qquad (5)$$

$$\partial_t \mathbf{u}_\perp = -(\mathbf{u}_\perp \cdot \nabla)\mathbf{u}_\perp - \nabla p + \frac{1}{Re}\nabla^2 \mathbf{u}_\perp - \frac{H}{Re}\mathbf{u}_\perp, \qquad (6)$$

where $\mathbf{u}_\perp$ and p are the velocity and pressure fields, respectively, in axial direction. The parameter $H = 2(L/a)^2 Ha$ is a measure of the friction term. All boundaries are assumed to be electrically insulated to ensure the validity of model being used. An advanced, high-order, in-house solver based on a spectral-element method for spatial discretization is employed to simulate the cases.

The numerical system has been validated for the wake of a circular cylinder for cases with and without a magnetic field. Further, a decaying line vortex based on the Lamb–Oseen solution has been simulated and compared with the analytical solution. Simulations were carried out at various different Hartmann number, circulation and initial core radius. Excellent agreement is seen between the numerical and analytical results. Further validation of the code can be found in [5, 4].

A grid independence study for spatial resolution has been performed by varying the element polynomial degree from 5 to 10, while keeping the macro element distribution unchanged. Meshes near the walls and the cylinder were refined to resolve the typical high gradients, especially with the flows involving strong magnetic fields. The pressure and viscous components of the time-averaged drag coefficient ($C_{D,p}, C_{D,\text{visc}}$) and the Strouhal frequency of vortex shedding (St) were monitored, as they are known to be sensitive to the domain size and resolution. Errors relative to the case with highest resolution, $\varepsilon_P = |1 - P_{Ni}/P_{N=10}|$, was defined as a monitor for each case, where P is the monitored parameter. A demanding MHD case with $Re = 8000$ and $Ha = 3750$ was chosen for the test. The results are presented in table 1, and show good convergence when the polynomial order increases. A mesh with polynomial degree 7 achieves at most a 0.1% error and is therefore used hereafter.

N_p	5	6	7	8	9
$\varepsilon_{C_{D,p}}$	0.0010	0.0002	0.0002	0.0002	0.0003
$\varepsilon_{C_{D,\text{visc}}}$	0.0024	0.0023	0.0010	0.0001	0.0000
ε_{St}	0.0034	0.0003	0.0002	0.0001	0.0000

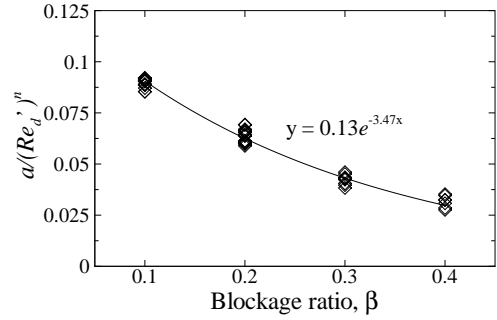Table 1: Grid independence study at $Re_L = 8000$ and $Ha = 3750$

Figure 2. Curve fitting for constant a. In the curve-fit equation, y is $a/(Re_d')^{1.44}$ and x is the blockage ratio, β.

Development of Correlation

It is observed from previous studies that increasing Hartmann number generally acts to increase the rate of vortex decay [5]. To quantify these observations, the peak vortex strength of wake vortices behind a cylinder has been recorded at a different blockage ratios and a broad range of Hartmann numbers and Reynolds numbers. These parameters are correlated by means of regression analysis. As a prelude to the current analysis, the influence of magnetic field on the decay of a single isolated vortex was considered as a basis for the functional form of the correlation, i.e. $\xi_{1,p} = a/(4t + b)$ and $\xi_p = ae^{-cHa\,t}/(4t + b)$ for pure hydrodynamic and magnetohydrodynamic cases, respectively. To obtain the values of constants a, b, and c, the time history of the peak vorticity within a single wake vortex as it advects downstream of a body is extracted from the simulations at blockage ratio between 0.1 and 0.4, Hartmann numbers between 250 and 2000, and Reynolds numbers based on channel half-height between 300 and 6000. The values of a and b were determined by curve-fitting the temporal decay of peak vortex strength for each hydrodynamic case ($Ha = 0$) into the aforementioned fitting function.

Inspection of the data for a range of parameters revealed that a is dependent on modified cylinder Reynolds number, $Re_d' = 2\beta Re_L/(1 - \beta)$ and blockage ratio, and b is dependent on channel Reynolds number, Re_L, blockage ratio and initial peak vortex strength, $\xi_{p,0}$. By plotting $a/(Re_d')^n$ against β and $b\xi_{p,0}/\beta$ against Re_L, the data collapse onto a curve described by exponential and power-law relations, respectively. figure 2 shows a typical plot, and regression analysis yields $a = 0.13e^{-3.47\beta}(Re_d')^{1.44}$ and $b = 0.092\beta Re_L^{1.46}/\xi_{p,0}$. Substitution into the fitting fucnction yields

$$\xi_p = \frac{0.13e^{-3.74\beta}\xi_{p,0}(Re_d')^{1.44}}{4\xi_{p,0}t + 0.092\beta(Re_L)^{1.46}}e^{-cHat}. \qquad (7)$$

Using the same approach as in the development of expressions for a and b for pure hydrodynamic flow, constant c was obtained from the peak vorticity time history of magnetohydrodynamic cases. It was then plotted against Re_L and the expression for c was obtained as $c = 2.32Re_L^{-1.02}$. Substitution into equation (7) gives

$$\xi_p = \frac{0.13e^{-3.74\beta}\xi_{p,0}(Re_d')^{1.44}}{4\xi_{p,0}t + 0.092\beta(Re_L)^{1.46}}e^{\left(-2.32\frac{Ha}{Re_L^{1.02}}t\right)}. \qquad (8)$$

This equation provides numerous insight into the temporal evolution of the wake vortices. First, the vortex decay in MHD is described by the power-law and exponential relationship. Equation (8) is re-written as $\xi_p = \xi_{p,\text{visc}} \times \xi_{p,H}$, where

$\xi_{p,\text{visc}} = 0.13\mathrm{e}^{-3.74\beta}\xi_{p,0}(Re'_d)^{1.44}/(4\xi_{p,0}t + 0.092\beta(Re_L)^{1.46})$ and $\xi_{p,H} = \mathrm{e}^{\left(-2.32Ha\,t/Re_L^{1.02}\right)}$ in order to emphasize the proportion of each damping force. $\xi_{p,\text{visc}}$ and $\xi_{p,H}$ correspond to viscous dissipation and magnetic damping, respectively. It is interesting to note that the rate of decay declines with time in a power function but remain constant in exponential function. This suggest that if the decay of the wake vortices is first dominated by the viscous dissipation, it will eventually be dominated by the magnetic damping. The threshold for this transition is when the decay rate for both damping force equalizes. However, at higher Hartmann number the magnetic damping effect already prevails from the beginning of the decay process. To illustrate this, figure 3 shows the effect of varying Hartmann number on the ratio of both damping contributions. It can be seen that in the absence of magnetic field, the curve of viscous-to-magnetic damping ratio decrease asymptotically to the x-axis (a typical power-law curve behaviour). However, in the presence of magnetic field, the curve turns to a positive gradient at a certain threshold (indicates by zero gradient). The turning point marks the beginning of the magnetic damping dominated region. For a given Reynolds number, the turning point shifted towards the y-axis as the Hartmann number increased, indicating shorter viscous dissipation dominated region. In the limiting case of high Hartmann number, the magnetic damping is already become the dominant forcing at the onset of vortex shedding (dashed curve). It is also important to note that this behaviour is a Reynolds number dependent, where higher Reynolds number tends to prolong the viscous dissipation dominated region.

Furthermore, the decay rate of peak vorticity depends on the initial peak vortex strength, which is consistent with Ponta's observation [8]. The decay rate is defined as the derivative of natural logarithm of peak vorticity in equation (8) with respect to time [5], i.e.

$$\frac{\partial(\log_e \xi_p)}{\partial t} = -2.32\frac{Ha}{Re_L^{1.02}} - \frac{4\xi_{p,0}}{4\xi_{p,0}t + 0.092\beta(Re_L)^{1.46}}. \quad (9)$$

As the time approaches infinity, the gradient of the decay rate curve reaches an asymptote at $-2.32Ha/Re_L^{1.02}$, an expression which closely resembles the Hartmann friction term in the governing equation (i.e. $-2Ha/Re_L$). This implies that the decay rate of peak vorticity approaches the Hartmann friction term at arbitrarily large time, which corroborates the aforementioned discussion.

Equation (8) also predicts peak vorticity time history for hydrodynamic flows by substituting $H = 0$, which yields

$$\xi_p = \frac{0.13\mathrm{e}^{-3.74\beta}\xi_{p,0}(Re'_d)^{1.44}}{4\xi_{p,0}t + 0.092\beta(Re_L)^{1.46}}. \quad (10)$$

Further, when unbounded flow is considered, i.e. $\beta = 0$, equation (10) recovers the inverse proportionality to time expected from the Lamb–Oseen vortex solution, i.e.

$$\xi_p = \frac{0.13(Re'_d)^{1.44}}{4t}. \quad (11)$$

Comparing equation (11) with the peak vorticity of the Lamb–Oseen vortex solution, i.e. $\xi_p = \Gamma/(4\pi\tau)$ yields

$$\Gamma = 0.13\pi Re_d^{0.44}. \quad (12)$$

This equation shows that circulation is a function of Reynolds number. Substituting $Re_d = 75$ results in $\Gamma = 2.7$, which is very close to values obtained from previous experimental data by [6]
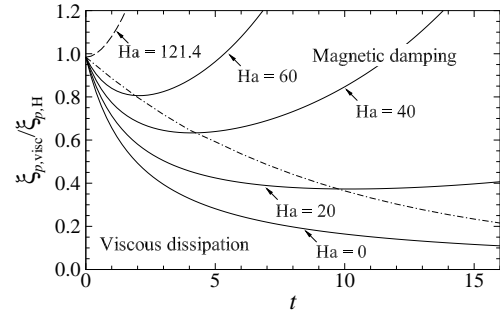

Figure 3. Time history of viscous-to-magnetic damping ratio for $Re_L = 500$. Negative slope indicates region dominated by viscous dissipation and positive slope indicates region dominated by magnetic damping. Zero gradient indicates threshold of MHD dominated region. The dash-dotted line connects the turning point of each curve, separating two dominating regions and crosses y-axis at $\xi_p(0)$. The data is normalized by the initial peak vorticity.
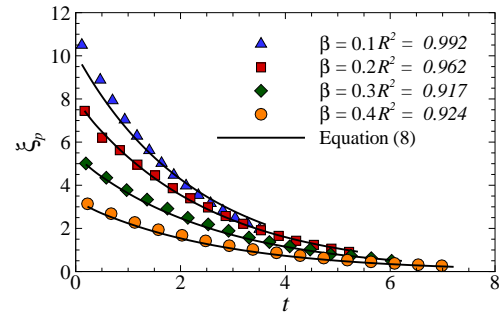

Figure 4. Decaying peak vorticity from numerical results and prediction by equation (8) for $Ha = 250$ and $Re_L = 1500$. R^2 represents the quality of the curve fit.

($\Gamma = 2.81$ for $Re_d = 75$). The small discrepancy may be due to the error in measuring velocity vectors in the experiment [6].

Correlation Validation

The validity of the devised correlations was examined using the current numerical data set. An overall correlation coefficient exceeding 90% was achieved, with more than 80% of the data set exceeding 95%. figure 4 represents a typical comparison between numerical results and prediction, and shows that the temporal evolution of peak vorticity at different blockage ratios are well predicted.

It should be emphasized that equation (8) should predict the peak vorticity well when the wake is stable, i.e. when the longitudinal spacing between two successive vortices, l is constant [1]. The spacing was determined by plotting the phase-downstream distance relationships along the wake, in which the typical plot can be found in [1]. The slope of the curve at any position will give the reciprocal of the longitudinal spacing of the vortices at that position. The plot shows that the longitudinal spacing became constant within two or three cylinder diameters downstream. Preceding the stable region is the formation region, where the vorticity dissipates and organises into a coherent structure in the vicinity of the cylinder [6]. This process can be further divided into three stages, namely the accumulation of vorticity from the separated boundary layers, the stretching of vorticity, and the seperation of this vorticity from the bound-
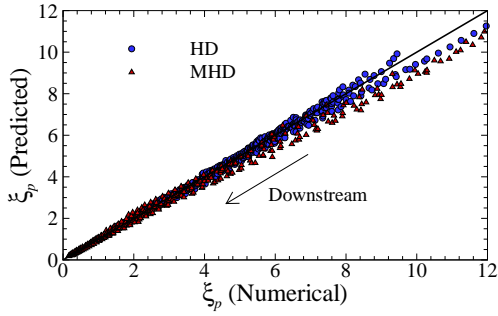
Figure 5. Overall comparison between numerical and predicted peak vorticity.
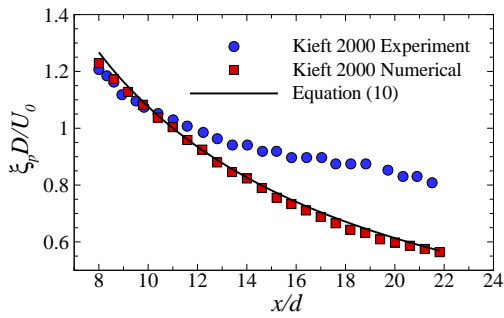

Figure 6. Comparison of predicted peak vorticity spatial evolution with the previous experimental data for $Re_d = 75$.

ary layer. This region consist of complex vortex geometries and behaviour and hence are not considered in the development of equation (8). This explains the scatter of data towards the stronger vorticity region seen in figure 5. As the wake moves further downstream, the wake stabilizes and hence equation (8) becomes more capable of predicting the peak vorticity, which produces the high collapse of data to a straight line of unit gradient as data approaches the origin. The accuracy of the devised correlation was further assessed by comparing the experimental and numerical results from [6] along with the predictions from equation (10), and is plotted in figure 6. The predictions compare very well with the numerical results, however deviation further downstream is seen in the experimental results. [6] attributes this discrepancy to the lower spatial resolution and noise in the experimental measurements.

Conclusion

The analytical solution for the decay of a line vortex in a quasi-two-dimensional MHD flow (analogous to the Lamb-Oseen solution for non-MHD flows) is obtained, and this forms the basis for a regression fit to describe the decay of wake vortices behind an idealized turbulence promoter (i.e. a circular cylinder) in a rectangular duct. The results show that at certain critical Hartmann numbers, magnetic damping becomes the dominant forcing for the decay of peak vortices. The correlation proposes that the decay rate varies with time, blockage ratio, imposed magnetic field intensity and Reynolds number. Asymptotically, the decay rate approaches approximately $-2Ha/Re$ at large times. It is also noted that although the Hartmann numbers studied are relatively small compared to fusion-relevant conditions, the magnetic field is already observed to significantly affect the wake vortices. Comparison with experimental and numerical data validates the capability of the devised correlation in predicting the decaying peak vortex intensity.

References

[1] Bearman, P., 1967, On vortex street wakes, *J. Fluid Mech*, **28**, 625–641.

[2] Bühler, L., 1996, Instabilities in quasi-two-dimensional magnetohydrodynamic flows, *Journal of Fluid Mechanics*, **326**, 125–150.

[3] Frank, M., Barleon, L. and Müller, U., 2001, Visual analysis of two-dimensional magnetohydrodynamics, *Physics of fluids*, **13**, 2287.

[4] Hussam, W. K. and Sheard, G. J., 2013, Heat transfer in a high hartmann number MHD duct flow with a circular cylinder placed near the heated side-wall, *International Journal of Heat and Mass Transfer*, **67**, 944–954.

[5] Hussam, W. K., Thompson, M. C. and Sheard, G. J., 2011, Dynamics and heat transfer in a quasi-two-dimensional MHD flow past a circular cylinder in a duct at high hartmann number, *International Journal of Heat and Mass Transfer*, **54**, 1091–1100.

[6] Kieft, R., 2000, *Mixed convection behind a heated cylinder*, Ph.D. thesis, Technische Universiteit Eindhoven.

[7] Polyanin, A. D., 2010, *Handbook of linear partial differential equations for engineers and scientists*, CRC press.

[8] Ponta, F. L., 2010, Vortex decay in the Kármán eddy street, *Physics of Fluids*, **22**, 093601.

[9] Pothérat, A., Sommeria, J. and Moreau, R., 2000, An effective two-dimensional model for MHD flows with transverse magnetic field, *Journal of Fluid Mechanics*, **424**, 75–100.

[10] Pothérat, A., Sommeria, J. and Moreau, R., 2005, Numerical simulations of an effective two-dimensional model for flows with a transverse magnetic field, *Journal of fluid mechanics*, **534**, 115–143.

[11] Sheard, G. J., Fitzgerald, M. J. and Ryan, K., 2009, Cylinders with square cross-section: wake instabilities with incidence angle variation, *Journal of Fluid Mechanics*, **630**, 43–69.

[12] Sommeria, J., 1988, Electrically driven vortices in a strong magnetic field, *Journal of Fluid Mechanics*, **189**, 553–569.

[13] Sommeria, J. and Moreau, R., 1982, Why, how, and when, MHD turbulence becomes two-dimensional, *Journal of Fluid Mechanics*, **118**, 507–518.